Journal of the European Ceramic Society **13** (1994) 121–127

The Dependence of the 'Relaxor' Type of Dielectric Response on Chemical Composition: A Study of Zirconium-Substituted Lead Magnesium Niobate

Andrew W. Tavernor & Noel W. Thomas*

School of Materials, University of Leeds, Leeds LS2 9JT, UK

(Received 26 July 1993; accepted 27 September 1993)

Abstract

Ceramics of lead magnesium niobium zirconium oxide, $Pb(Mg_{(1-x)/3}Nb_{2(1-x)/3}Zr_x)O_3$ $(0 \leq x \leq 0.3)$, have been fabricated and characterised, with 'relaxor' ferroelectric properties shown by all compositions. Samples have been prepared in a two stage 'mixed oxide' synthesis, with XRD studies confirming the existence of a solid solution for each composition in the range. A full dielectric characterisation has been carried out, with measurements made of ε_r' and ε_r'' versus temperature at five different frequencies between 100 Hz and 1 MHz.

The variation of dielectric response with zirconium concentration, x, is described through the use of four empirical parameters, $T(\varepsilon_{r,max}')$, $\varepsilon_{r,max}'$, δ and $\Delta T'$, which are derived from the variation of ε_r' with temperature. A rationalisation of the observed trends is given, employing the 'polarisation cluster' conceptual framework. Consideration of the properties of NbO_6, MgO_6 and ZrO_6 cation coordination polyhedra permits an understanding of the compositional dependence of the 'relaxor' response, which is helpful in the design of new compositions with desirable dielectric properties. The dielectric behaviour of the related system $Pb(Mg_{(1-x)/3}Nb_{2(1-x)/3}Ti_x)O_3$ can also be understood in these terms.

Die hergestellten und untersuchten Blei-Magnesium-Niob-Zirkoniumoxid-Keramiken $Pb(Mg_{(1-x)/3}Nb_{2(1-x)/3}Zr_x)O_3$ $(0 \leq x \leq 0.3)$ zeigten alle 'relaxor' ferroelektrisches Verhalten. Die Proben wurden in einer zweistufigen 'mixed oxide' Synthese hergestellt. XRD-Untersuchungen bestätigten das Vorhandensein eines Mischkristalls für jede Zusammensetzung innerhalb des betrachteten Bereichs. Die dielektrischen Konstanten ε_r' und ε_r'' wurden als Funktion der Temperatur bei fünf verschiedenen Frequenzen zwischen 100 Hz und 1 MHz gemessen.

Das dielektrische Verhalten in Abhängigkeit vom Zirkoniumgehalt x kann durch vier empirische Parameter, $T(\varepsilon_{r,max}')$, $\varepsilon_{r,max}'$, δ und $\Delta T'$, beschrieben werden. Diese lassen sich aus der Variation von ε_r' mit der Temperatur ableiten. Das beobachtete Verhalten kann mit Hilfe des 'polarisation cluster' Konzepts erklärt werden. Die Betrachtung der Eigenschaften der NbO_6-, MgO_6- und ZrO_6-Kationenkoordinationspolyeder erlaubt die Abhängigkeit des 'relaxor' Verhaltens von der Zusammensetzung zu verstehen. Dies ist hilfreich bei der Entwicklung neuer Zusammensetzungen mit gewünschten, dielektrischen Eigenschaften. Das dielektrische Verhalten des verwandten Systems $Pb(Mg_{(1-x)/3}Nb_{2(1-x)/3}Ti_x)O_3$ läßt sich in gleicher Weise verstehen.

On a élaboré et caractérisé des céramiques d'oxyde de plomb, de magnésium, de niobium et de zirconium ($Pb(Mg_{(1-x)/3}Nb_{2(1-x)/3}Zr_x)O_3$ $(0 \leq x \leq 0.3)$, toutes les compositions choisies présentent des propriétés ferroélectriques 'd'oscillateur à relaxation'. On a préparé les échantillons par une synthèse 'd'oxydes mixtes' en deux étapes, des mesures de diffraction X permettant de confirmer l'existence d'une solution solide pour chaque composition. On a procédé à une caractérisation diélectrique complète, avec mesure de ε_r' et ε_r'' en fonction de la température à cinq fréquences différentes comprises entre 100 Hz et 1 MHz.

On décrit la variation de la réponse diélectrique avec x, concentration en zirconium, à l'aide de quatre paramètres empiriques, $T(\varepsilon_{r,max}')$, $\varepsilon_{r,max}'$, δ et $\Delta T'$, qui proviennent de la variation de ε_r' avec la température. On rationalise les tendances observées dans le cadre du concept 'd'amas de polarisation'. En s'attachant aux propriétés des polyèdres de coordination cation-

* To whom correspondence should be addressed

ques NbO_6, MgO_6 et ZrO_6, on peut comprendre d'où provient la dépendance en composition de la réponse ferroélectrique en 'oscillateur à relaxation', ceci devrait de mieux choisir de nouvelles compositions présentant les propriétés diélectriques voulues. On peut aussi interpréter en ces termes le comportement du système voisin $Pb(Mg_{(1-x)/3}Nb_{2(1-x)/3}Ti_x)O_3$.

1 Introduction

A general technique for investigating relaxor ferroelectric ceramics is to carry out a partial substitution of the cations in a parent, model relaxor composition with foreign cations, and to monitor the effect on the dielectric properties. In this context, novel work is presented here on the synthesis and characterisation of the perovskite (ABO_3) system zirconium-substituted lead magnesium niobate. Here the B ion sites (occupied by Mg^{2+} and Nb^{5+} ions in the parent composition) are partly occupied by Zr^{4+} ions, to give $Pb(Mg_{(1-x)/3}Nb_{2(1-x)/3}Zr_x)O_3$. It is seen from this formula that the B-ion sites in the zirconium-substituted composition are fully occupied, as in the parent composition. Further, it is convenient to employ the acronym PMNZ-x for this system, where x represents the fraction of perovskite B-sites occupied by zirconium ions. Values of x in this study lie in the range $0 \leq x \leq 0{\cdot}3$. Note that the universally accepted acronym for the parent composition, $Pb(Mg_{1/3}Nb_{2/3})O_3$, is PMN.

Apart from the obvious application of high-permittivity relaxor ceramics in capacitors, increasing utilisation of these materials is to be found in electrostrictive devices, where their large electric-field induced polarisations are associated with a mechanical strain. Since the subsequent development of electrostrictive ceramics will embrace both compositional and microstructural factors, the compositionally based approach developed in this paper represents an applicable strategy for optimising the properties of these materials.

2 Experimental

2.1 Powder synthesis

Powders of PMNZ-x were synthesised from proprietary powders of PbO, $(MgCO_3)_4Mg(OH)_2 \cdot 5H_2O$/MgO, Nb_2O_5 and ZrO_2, using a 'mixed oxide' route. Two alternative two stage routes were evaluated, with the twin aims of minimising the formation of a lead niobium oxide pyrochlore phase[1] and identifying the optimum method for incorporating zirconium ions homogeneously into the perovskite structure.

The two routes are designated 1 and 2:

Route 1

$$(1-x)MgO + (1-x)Nb_2O_5 + 3xZrO_2 \rightarrow Mg_{1-x}Nb_{2(1-x)}Zr_{3x}O_6$$

$$3PbO + Mg_{1-x}Nb_{2(1-x)}Zr_{3x}O_6 \rightarrow 3Pb(Mg_{(1-x)/3}Nb_{2(1-x)/3}Zr_x)O_3$$
$$(x = 0, 0{\cdot}01, 0{\cdot}05, 0{\cdot}10)$$

Route 2

$$(MgCO_3)_4\ Mg(OH)_2 \cdot 5H_2O + 5Nb_2O_5 \rightarrow 5MgNb_2O_6$$

$$3PbO + (1-x)MgNb_2O_6 + 3xZrO_2 \rightarrow 3Pb(Mg_{(1-x)/3}Nb_{2(1-x)/3}Zr_x)O_3$$
$$(x = 0, 0{\cdot}01, 0{\cdot}05, 0{\cdot}10, 0{\cdot}20, 0{\cdot}30)$$

In essence, zirconia is reacted in the first stage in Route 1 and in the second stage in Route 2. Although MgO is employed in the first route and $(MgCO_3)_4Mg(OH)_2 \cdot 5H_2O$ in the second, this is not thought to be a significant difference, since comparable PMN samples can be made from either starting reagents.

Since a Route 1 type of mechanism had been found to be successful in the synthesis of $Pb(Mg_{1/3}Nb_{2/3})O_3$-$PbTiO_3$ (PMN-PT) ceramics,[2] it was hoped that this method would provide a uniform distribution of Zr within the columbite structure (that of $MgNb_2O_6$). This should favour, in turn, a homogeneous distribution of Zr ions within the perovskite PMNZ-x phase.

Route 2, by comparison, involves the formation of columbite, $MgNb_2O_6$, prior to reaction with PbO and ZrO_2. It is therefore more convenient for the synthesis of a range of compositions from a single batch of $MgNb_2O_6$. This type of reaction sequence has also been successfully applied to the synthesis of PMN-PT compositions.[3]

Starting powders were ball-milled in acetone using zirconia media for 24 h, in order to achieve intimate mixing. Following solvent evaporation, the first calcination was carried out at 1050°C for 4 h. Subsequent calcination to form the perovskite PMNZ-x phase was carried out at 800°C for 2 h.

2.2 Ceramic fabrication

A standard pseudo double-ended uniaxial die pressing technique (10 mm diameter, 80 MPa pressure, 5 min) was used to press the powders into green pellets. To aid pressing and green densification, polymeric binders and plasticisers were added (0·25 wt% PVA and 0·75 wt% PEG respectively), in optimum amounts which were determined empirically.[4] These additives were burnt off at 450°C for a period of 4 h. Furnace ramp rates were $\leq 2°C\ h^{-1}$, in

order to reduce the risk of porosity or lamination caused by sudden burn-out. All pellets were densified by sintering at 1220°C for 2 h.

2.3 Preparation and measurement of dielectric specimens

Single phase samples of comparable density (in excess of 98.5% of theoretical density) were selected for dielectric measurements. The sintered pellets were ground and polished down to parallel-sided disks of thickness 200 μm and ultrasonically cleaned in acetone. Gold electrodes were sputtered on to both faces, which were subsequently covered with air drying silver paint. Complex impedance measurements were taken over 5 decades of frequency (100 Hz to 1 MHz) from −75°C to 100°C using an HP4284A precision LCR meter in conjunction with a Delta Design 9023 environmental test chamber. The system was operated remotely from a personal computer, using software developed at Leeds.

3 Results

3.1 X-ray diffraction analysis

The X ray diffraction patterns (Siemens Kristalloflex 805 diffractometer with DIFFRAC 500 software) obtained from both powders and sintered ceramics are given in Fig. 1. Figures 1(a) and (b) refer to Route 1 and Fig. 1(c) and (d) to Route 2.

It is seen in Fig. 1(a) that the zirconium ions have only limited solubility in the parent $MgNb_2O_6$ columbite phase: there is a small shift of the diffraction peaks to lower angles of the peaks in going from $x = 0$ to $x = 0.01$ in $Mg_{1-x}Nb_{2(1-x)}Zr_xO_6$, indicative of a small increase in unit cell size upon substitution Zr^{4+} for Mg^{2+} and Nb^{5+}. However, the dominant feature upon addition of zirconium ions is the appearance of extra diffraction peaks corresponding to ZrO_2 as a second phase. Most noticeable is the peak at $d = 3.157$ Å, interpreted as the ZrO_2 peak with the highest intensity.

Figure 1(b) shows the diffraction patterns obtained for PMNZ x powders ($x = 0.01$, 0.05, 0.10), following the second calcination of Route 1. In general, these do not correspond to single phases or solid solutions. Note the presence of a large pyrochlore peak at $d = 2.91$ Å, even in the $x = 0$ composition, where the diffraction pattern of the corresponding precursor $x = 0$ columbite phase (Fig. 1) is satisfactory.

Figure 1(c) and (d) give diffraction patterns for PMNZ x compositions in powder and sintered form respectively, as produced by Route 2. Figure 1(c) contains evidence of small amounts of second phases, in amounts apparently uncorrelated with the

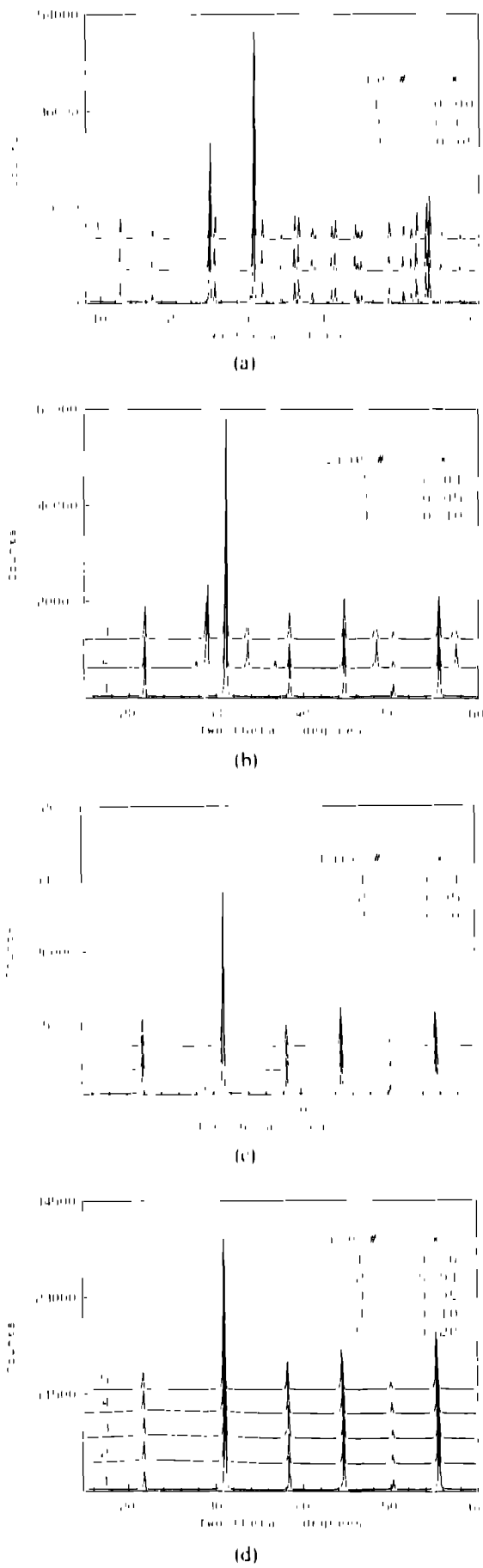

Fig. 1. X ray diffraction patterns corresponding to (a) the compositions $Mg_{1-x}Nb_{2(1-x)}Zr_xO_6$, for $x = 0$, 0.01 and 0.05, (b) PMNZ x powders produced by Route 1, for $x = 0.01$, 0.05 and 0.10, (c) PMNZ x powders produced by Route 2, for $x = 0.01$, 0.05 and 0.10, (d) sintered PMNZ x samples produced by Route 2, for $x = 0$, 0.01, 0.05, 0.10 and 0.20

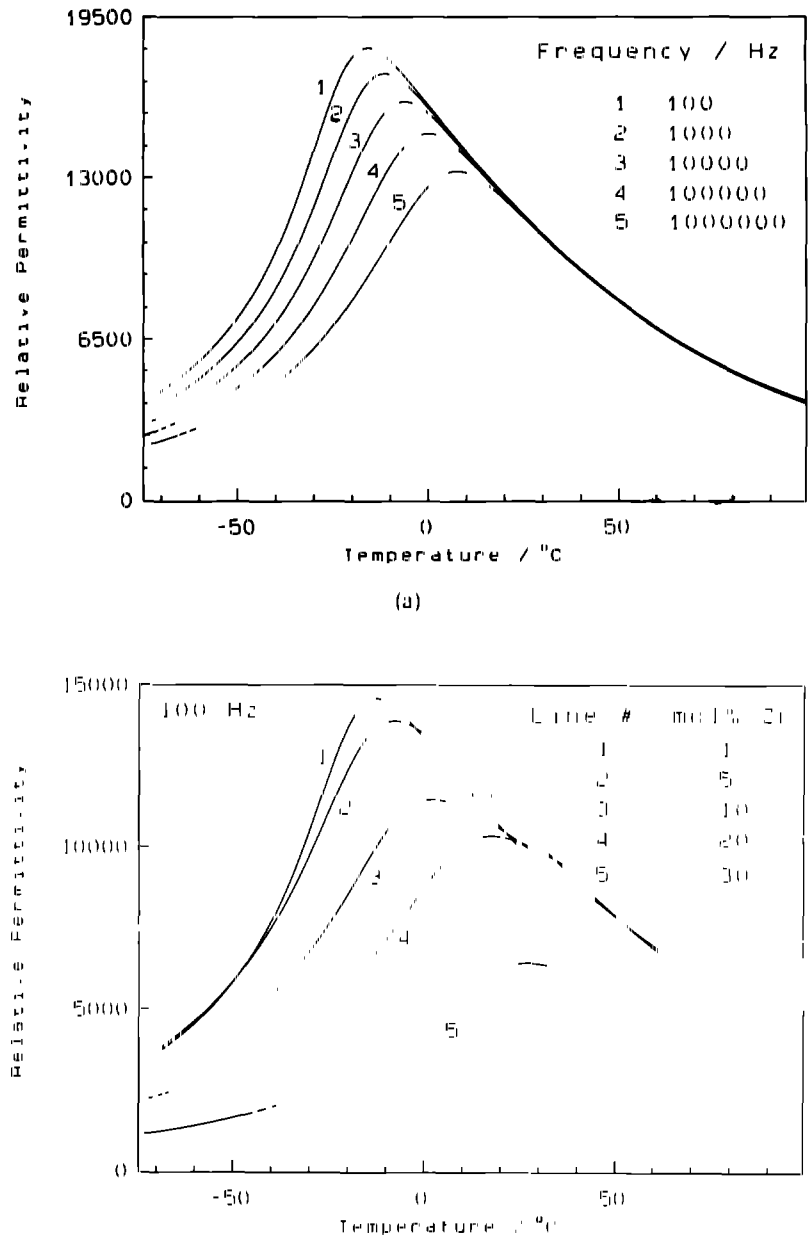

Fig. 2. Variation with temperature of relative permittivity ε_r' for PMNZ x ceramics synthesised by Route 2. (a) The influence of frequency is shown for a sample with $x = 0$. Similar influence is observed for samples with other x values. (b) The influence of x value in measurements made at 100 kHz. The compositions are $x = 0.01, 0.05, 0.1, 0.2$ and 0.3.

value of x. Following remilling and sintering, these second phases disappear, to give rise to diffraction patterns as in Fig. 1(d). It should be noted here that the diffuse amorphous peak at low angles is a consequence of the glass sample holder and not of the samples themselves.

Route 2 is therefore the more successful method of producing PMNZ x, as verified in Fig. 1(d) for values of x up to 0·20. The parent phase ($x = 0$) was found to correspond exactly to the known PMN phase (JCPDS data file 22-1199). Upon zirconium substitution, all the peaks are shifted to slightly smaller angles, indicative of a small increase in unit cell size. Thus the X-ray evidence points towards the formation of a solid solution in the range $0 \leq x \leq 0.2$.

3.2 Dielectric measurements

Figure 2(a)–(f) gives the measured variation with temperature and frequency of relative permittivity (ε_r') for PMNZ-x ceramics ($x = 0, 0.01, 0.05, 0.1, 0.2$ and 0.3) synthesised by Route 2. In order to focus attention on the dependence of key parameters of the dielectric response upon composition, some features of the data for 100 kHz (the lowest measurement frequency) are highlighted in Figs 3 to 5. More specifically, Fig. 3 gives a plot of the variation of the temperature of maximum relative permittivity, $T(\varepsilon_{r,max}')$, with x. Figure 4 gives the variation of the magnitude of the maximum permittivity, $\varepsilon_{r,max}'$, with Fig. 5 a compilation of dielectric loss curves at 100 Hz.

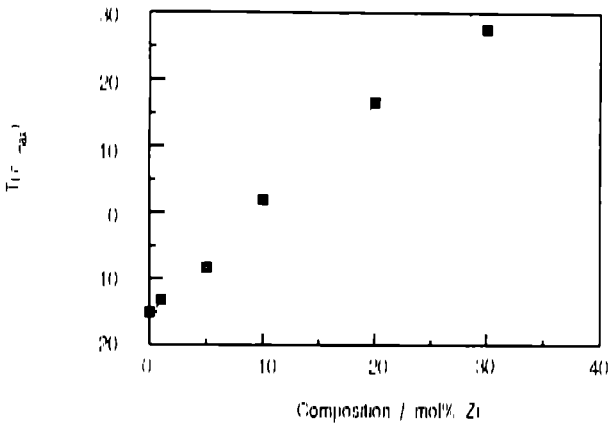

Fig. 3. Dependence of $T(\varepsilon'_{r,max})$ on x in PMNZ x

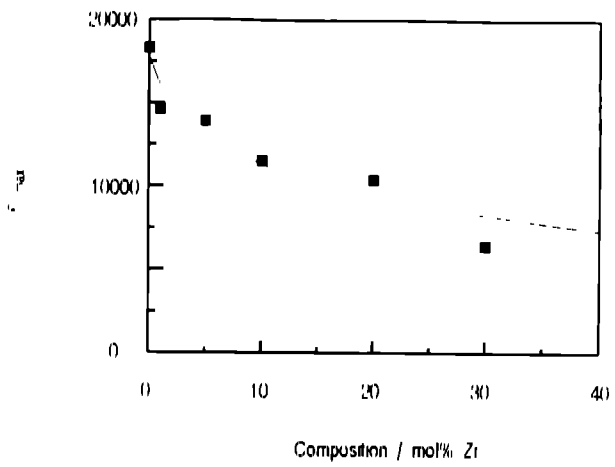

Fig. 4. Dependence of $\varepsilon'_{r,max}$ on x in PMNZ x

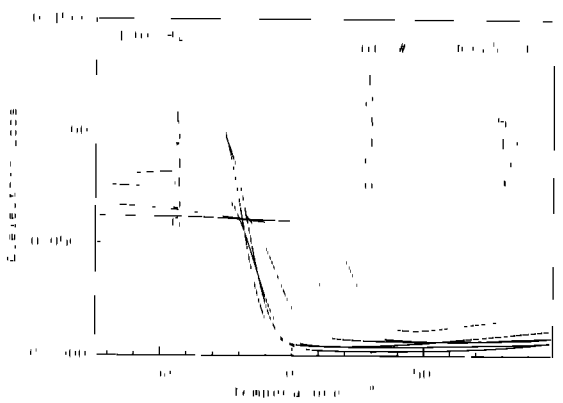

Fig. 5. Dependence of $\varepsilon''_{r,max}$ on x in PMNZ x

It is seen in Fig. 3 that $T(\varepsilon'_{r,max})$ increases uniformly with x in a variation which tends towards linearly $\varepsilon'_{r,max}$, however, falls with x non-linearity, as indicated in Fig. 4 by the approximate curve. As regards dielectric loss, Fig. 5 shows that there is a general reduction in ε''_r with x.

Three further parameters, δ, γ and $\Delta T'$, are invoked to quantify the variation of ε'_r with temperature and frequency, with the values of these quoted in Table 1. The first of these, δ, was introduced by Kirillov & Isupov[5] to quantify the 'diffuseness' of a given $\varepsilon'_r(T)$ maximum. According to this parametrisation, the following general relationship applies

$$\frac{1}{\varepsilon'_r} - \frac{1}{\varepsilon'_{r,max}} = \frac{(T - T_{\varepsilon'_{r,max}})^2}{2\varepsilon'_{r,max}\delta^2} \qquad (1)$$

The second parameter, γ, termed 'critical exponent', relates to an alternative parametrisation proposed by Uchino & Nomura[6]

$$\frac{1}{\varepsilon'_r} - \frac{1}{\varepsilon'_{r,max}} = \frac{(T - T_{\varepsilon'_{r,max}})^\gamma}{C} \qquad (2)$$

The exponent γ lies in the range $1 \leq \gamma \leq 2$, tending to 1 for a normal (i.e. non diffuse) ferroelectric and rising towards 2 for a relaxor.

In the current work, δ and γ are regarded as independent indicators of diffuseness, with a third parameter, $\Delta T'$, utilised to quantify directly the degree of relaxation behaviour

$$\Delta T' = T_{\varepsilon'_{r,max}\,1\,MHz} - T_{\varepsilon'_{r,max}\,100\,Hz} \qquad (3)$$

$\Delta T'$ quantifies the observable relaxor properties explicitly the extent to which the dielectric maxima are shifted to higher temperatures with increasing frequency.

From Table 1 it is seen that both δ and γ rise in the composition range $x = 0$ to $x = 0.20$, indicating a progressive increase in diffuseness, with both δ and γ values falling off between $x = 0.20$ and $x = 0.30$. The $\Delta T'$ parameter reaches a maximum for the $x = 0.01$ composition, falling off at larger values of x. Thus the predominant trend is that zirconium substitution reduces the degree of relaxation behaviour.

Table 1. δ, γ and ΔT for PMNZ x ceramics

Composition (x)	δ (K)	γ	ΔT (K)
0.00	43.66	1.54	23.70
0.01	46.37	1.63	27.30
0.05	49.29	1.69	26.37
0.10	52.80	1.78	25.00
0.20	55.30	2.13	19.80
0.30	53.76	1.56	18.21

4 Discussion

4.1 Crystal structural considerations

The increase in unit cell size with increasing x (Fig. 1(d)) is to be expected from considerations of the relevant six fold coordinated ionic radii[7] $r^{VI}(Mg^{2+}) = 0.72$ Å, $r^{VI}(Zr^{4+}) = 0.72$ Å, $r^{VI}(Nb^{5+}) = 0.64$ Å, and $r^{XII}(Pb^{2+}) = 1.49$ Å.

From the formula of PMNZ x, $Pb(Mg_{(1-x)/3}Nb_{2(1-x)/3}Zr_x)O_3$, these ionic radii give rise to the following predicted (idealised) cubic cell parameter, a_0

$$a_0(\text{Å}) = 4.053\,33 + 0.106\,66x \qquad (4)$$

Straightforward application of the Bragg equation reveals that the observed shifts to lower angle upon Zr^{4+} substitution are consistent with the above variation in a_0.

4.2 The variation of dielectric response with x

The above results concerning dielectric response can be summarised in the following four trends:

(i) Upon the substitution of zirconium ions in PMN, $T(\varepsilon'_{r\,max})$ rises (Fig. 3).

(ii) As zirconium ions are introduced into PMN, $\varepsilon'_{r\,max}$ falls from a value in excess of 18 000 for $x = 0$ to approximately 6500 for $x = 0{\cdot}3$ (Fig. 4).

(iii) The diffuseness, δ, shows an overall increase from 43.66 K in the $x = 0$ composition to 53.76 K for $x = 0.3$ (Table 1).

(iv) The degree of relaxation behaviour, $\Delta T'$, shows an overall decrease from 23.70 K for $x = 0$ to 18.21 K for $x = 0.3$ (Table 1).

In connection with the first trend, it is clear that the zirconium ion, Zr^{4+} is effective in stabilising the polarisation within the polarisation clusters of the relaxor to a higher temperature than in the parent composition, PMN. This may be attributed to the probable distortion of the oxygen octahedron coordinating the zirconium ions, as shown in Fig. 6. This type of distortion, in which the upper triangular face of oxygen ions becomes larger than the lower triangular face, is commonly found in rhombohedral perovskites.[8] The unequal edge lengths in the triangles permit a relatively large ion, such as Zr^{4+}, to be displaced from the centre of coordinates of the O_6 octahedral cage towards the larger face, thereby creating an electric dipole moment.

Such ZrO_6 dipoles could act as structural units which would be stable to higher temperatures than their NbO_6 counterparts. Furthermore, these ZrO_6 octahedra would favour the parallel (ferroelectric) alignment of neighbouring NbO_6 dipoles, through electrostatic interactions. The persistence of the polar ZrO_6 octahedra to higher temperatures would thus provide a mechanism for stabilising neighbouring NbO_6 dipoles to higher temperatures than in the parent composition. The associated polarisation clusters would consequently be stable to higher temperatures, with a predicted increase in $T(\varepsilon'_{r,max})$ with x.

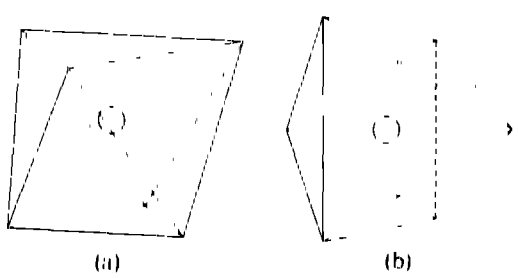

Fig. 6. The anticipated rhombohedral distortion of the ZrO_6 cation coordination polyhedron (a) in clinographic projection; (b) viewed along the trigonal three fold axis.

Since the parent composition, PMN, is characterised by a small rhombohedral distortion, it is likely that the MgO_6 octahedra will exhibit similar distortions to those postulated for ZrO_6 units. Note from Fig. 6 how three-fold symmetry is maintained in these distortions. From geometrical considerations alone, it is to be expected that MgO_6 and ZrO_6 octahedra will have comparable distortions, since Mg^{2+} and Zr^{4+} ions have identical ionic radii. However, the smaller formal charge on Mg(+2) compared to Zr(+4) implies that the magnitudes of the MgO_6 dipole moments will be considerably smaller. The MgO_6 octahedra will thus be less effective in providing dipoles with which coordinating NbO_6 dipoles can be aligned. The smaller charge of the magnesium ion implies that it will also be less effective than zirconium in polarising the electrons of coordinating oxygen ions. In general, metal–oxygen interactions of this kind, corresponding to incipient covalency, are crucial to the stabilisation of polar MO_6 octahedra to higher temperatures.

Trend (ii) reveals that, although substitution of Zr^{4+} ions raises $T(\varepsilon'_{r,max})$, there is an associated decrease in permittivity values, ε'_r. Thus the parameters $T(\varepsilon'_{r,max})$ and $\varepsilon'_{r,max}$ vary essentially independently of each other in this case.

For a given concentration, x, of Zr^{4+} ions in PMNZ-x, the concentrations of Mg^{2+} and Nb^{5+} ions are $(1-x)/3$ and $2(1-x)/3$. Thus twice as many Nb^{5+} ions are replaced by the Zr^{4+} ions as Mg^{2+} ions. As has been argued previously for PMN,[9] the NbO_6 octahedra are the principal constituents of the polarisation clusters, with the MgO_6 octahedra responsible for creating the clustered structure, rather than one made up of the ferroelectric domains with long-range dipolar coupling. In forming substituted compositions PMNZ-x, a structure based on polarisation clusters is maintained, along with the associated relaxor response. However, since the polarisability of NbO_6 octahedral units will be greater than that of ZrO_6 octahedra, the reduction in Nb^{5+} concentration is expected to lead to an overall reduction in values of $\varepsilon'_{r,max}$.

The third trend, relating to the diffuseness of the maximum in ε'_r, reflects the greater range in the chemical composition of the polarisation clusters PMNZ-x solid solutions compared to the parent PMN. Those clusters with a relatively greater zirconium content will give a large contribution to the dielectric response at a higher temperature than those regions with a lower Zr^{4+} concentration.

Trend (iv) shows that zirconium substitution

affects diffuseness and the degree of relaxation behaviour differently. In reducing the concentration of Mg^{2+} ions, the degree to which the MgO_6 octahedra in break up long-range dipolar coupling will be reduced.

The third trend, relating to diffuseness, is worthy of further consideration. In the system PMNZ-x, the diffuseness increases as an extra chemical component, Zr^{4+}, is added. However, this is not always the case, as for example in the related system, PMNT-x, $Pb(Mg_{(1-x)/3}Nb_{2(1-x)/3}Ti_x)O_3$. Here the Mg and Nb ions are replaced by the smaller Ti^{4+} ion ($r^{VI}(Ti^{4+}) = 0.605$ Å), with the polarisability of TiO_6 octahedra considerably greater than their ZrO_6 counterparts. In this system, the diffuseness is reduced as Ti^{4+} is added. The PMNT-x system has been investigated by several workers,[3] with values for δ, γ and $\Delta T'$ obtained from samples prepared in this laboratory (Table 2).[4]

The opposite trends in the variation of diffuseness with x between PMNZ-x and PMNT-x imply that a consideration of chemical inhomogeneity on a strict proportional basis i.e. at a unit cell level, is insufficient to rationalise the dielectric response. Rather, the overall compositions of larger structural entities such as polarisation clusters should be taken into account.

It is argued, therefore, that the introduction of Ti^{4+} ions gives rise to larger polarisation clusters than in PMNZ-x, since the TiO_6 dipoles are more effective than the ZrO_6 units in overcoming the clustering effect of the magnesium ions. This viewpoint is supported by the more sudden drop in $\Delta T'$ values with increasing x (cf. Tables 1 and 2). As the average size of these clusters increases, the extent of the variation in overall chemical composition between them is reduced, leading to sharper maxima in ε_r'. This rationalisation is further supported by data on PMNT-x for values of $x < 0.3$.[3] At $x \approx 0.4$, a phase transition to a tetragonal ferroelectric phase takes place, which exhibits a sharp ε_r' maximum characteristic of a normal ferroelectric. It is probable that conventional ferroelectric domains are formed in this tetragonal phase, unlike the case at lower substitutional levels in the rhombohedral phase, where relaxor behaviour is still observed.

Table 2. δ, γ and ΔT for PMNT-x ceramics

Composition (x)	δ(k)	γ	ΔT(k)
0.00	43.66	1.54	23.70
0.02	36.06	1.72	21.30
0.05	33.51	1.57	18.40
0.10	31.46	1.68	15.80
0.20	29.42	1.61	7.80

5 Conclusion

The system PMNZ-x has been found to exhibit more diffuse maxima in its ε_r' versus T variation than its parent composition, PMN. Despite the lower values of ε_r', this more diffuse behaviour (temperature stability of response), coupled with smaller values of dielectric loss, ε_r'', make this system a strong candidate for capacitative applications at ambient temperatures.

An interpretation of the variation in dielectric response with increasing zirconium substitution has been given in terms of a conceptual framework involving polarisation clusters made up of BO_6 dipoles. The anticipated properties of NbO_6, MgO_6, ZrO_6 and TiO_6 octahedra have been discussed, with a rationalisation given for the dissimilarities between PMNZ-x and PMNT-x.

References

1. Swartz, S. L. & Shrout, T. R., Fabrication of perovskite lead magnesium niobate. *Mat. Res. Bull.*, **17** (1982) 1245–50.
2. Hilton, A. D., Randall, C. A., Barber, D. J. & Shrout, T. R., TEM studies of $Pb(Mg_{1/3}Nb_{2/3})O_3$–$PbTiO_3$ ferroelectric relaxors. *Ferroelectrics*, **93** (1989) 379–86.
3. Choi, S. W., Shrout, T. R., Jang, S. J. & Bhalla, A. S., Dielectric and pyroelectric properties in the $Pb(Mg_{1/3}Nb_{2/3})O_3$–$PbTiO_3$ system. *Ferroelectrics*, **100** (1989) 29–38.
4. Tavernor, A. W., Modelling relaxor ferroelectrics. PhD Thesis, University of Leeds, UK, 1992.
5. Kirillov, V. V. & Isupov, V. A., Relaxation polarization of $PbMg_{1/3}Nb_{2/3}O_3$ (PMN)—a ferroelectric with a diffused phase transition. *Ferroelectrics*, **5** (1973) 3–9.
6. Uchino, K. & Nomura, S., Critical exponents of the dielectric constants in diffused phase transition crystals. *Ferroelectrics Lett.* **44** (1982) 55–61.
7. Shannon, R. D., Revised effective ionic radii and systematic studies of interatomic distances in halides and chalcogenides. *Acta Cryst.* **A32** (1976) 751–67.
8. Thomas, N. W. & Beitollahi, A., submitted to *Acta Cryst.* **B**.
9. Thomas, N. W., A new framework for understanding relaxor ferroelectrics. *J. Phys. Chem. Solids*, **51** (1990) 1419–31.